Copper Excess Reduces the Fluidity of Plasma Membrane Lipids of Wheat Roots: a Spin Probe EPR Study

Lucia Calucci and Calogero Pinzino*

Istituto per i Processi Chimico-Fisici, CNR, Area della Ricerca di Pisa, via G. Moruzzi 1, 56124, Pisa, Italy

Mike F. Quartacci and Flavia Navari-Izzo

Dipartimento di Chimica e Biotecnologie Agrarie, Università degli Studi di Pisa, via del Borghetto 80, 56124, Pisa, Italy

Received: April 11, 2003; In Final Form: July 24, 2003

Electron paramagnetic resonance spectroscopy was applied to investigate changes in the organization and dynamics of plasma membrane (PM) lipids of roots caused by growing wheat (*Triticum durum* Desf. cv. Creso) seedlings under copper excess (50 μM Cu^{2+}). To this purpose, unilamellar vesicles were made from total lipid extracts of PMs isolated either from copper-stressed or control roots, and probed at different bilayer depth using stearic acids bearing a doxyl group at two different positions of the alkyl chain, namely at the fifth (5-DSA) and 16th (16-DSA) carbon. EPR spectra were recorded as a function of temperature in the range between 273 and 323 K and interpreted in terms of a microscopically ordered and macroscopically disordered model, in which orientational ordering and dynamics of the spin probes were described by means of the order parameter *S* and the rotational diffusion coefficient *R*, respectively. It was found that growth in Cu excess resulted in a decreased root PM fluidity. The results were discussed in relation to the changes observed in the lipid composition of PMs induced by Cu stress, paying particular attention to phosphatidylcholine/phosphatidylethanolamine and phospholipids/free sterols ratios and to fatty acyl chain unsaturation degree of phospholipids.

Introduction

Copper is an essential micronutrient for normal plant growth and development, being an indispensable element of membrane-bound redox components and several oxidative enzymes of cells.[1] However, when present in excess, Cu can also be a toxic element inducing alterations in several biochemical and physiological processes.[2] In particular, Cu is known to damage cell membranes by binding to the sulfydryl groups of membrane proteins[3] and by inducing lipid peroxidation.[4,5] In fact, Cu is a redox active metal that can catalyze the formation of harmful free radicals such as hydroxy, peroxy, and alkoxy radicals in Fenton-type reactions and may therefore cause oxidative stress in cells.[6]

The root cell plasma membrane (PM) may be regarded as the first living structure of plants in contact with toxic metals; as such it is the first target for heavy metal toxicity, but it can also play a critical role in plant metal tolerance.[2] PM lipid composition contributes to the control of membrane packing properties and influences protein−lipid interactions, thus affecting membrane permeability and its efficiency as a semipermeable barrier.[7] Plant cell membranes are dynamic structures extremely sensitive to changes in their chemical and physical environment.[8−11] Alterations in membrane lipid composition represent one of the main mechanisms for plant cell adaptation to new environmental conditions.

In a previous work, it was found that growth of wheat seedlings in copper excess (50 μM Cu^{2+}) resulted in an altered lipid composition of PMs of root cells.[5] In particular, the phosphatidylcholine/phosphatidylethanolamine (PC/PE) ratio and the fatty acyl unsaturation degree (reported as the double bond index, DBI) decreased, whereas the phospholipids/free sterols (PL/FS) ratio increased in comparison with the control (PMs of seedlings supplied with 0.3 μM Cu^{2+}) (see Table 1). Unilamellar vesicles made from total lipid extracts of isolated PMs of copper-stressed roots (sample S) showed a remarkably lower permeability to glucose than vesicles made from lipids extracted from PMs of control roots (sample C), whereas no differences were observed in proton permeability.[12,13] A spin probe EPR study corroborated these findings, showing that at room temperature (298 K) the S vesicles have a lower fluidity than the C ones.[13]

TABLE 1: Phosphatidylcholine to Phosphatidylethanolamine (PC/PE) and Phospholipids to Free Sterols (PL/FS) Molar Ratios and Double Bond Index (DBI) of Vesicles

sample	PC/PE	DBI	PL/FS
C	0.7	2.1	1.8
C + PE	0.4	1.7	2.4
S	0.3	0.9	2.6
S + PC	0.5	2.0	3.2

However, in that study, a quite crude measure of the spin probes mobility was performed, and a single temperature was considered. Here, EPR spectroscopy is employed to more carefully investigate lipid organization and dynamics in S and C vesicles, performing measurements over a wide temperature range (273−323 K) and analyzing spectra quantitatively. To this purpose, lipid vesicles were doped with stearic acids bearing

* Corresponding author: Phone: +39-50-3152460. Fax: +39-50-3152442. E-mail: rino@ipcf.cnr.it.

10.1021/jp034980w CCC: $25.00
Published on Web 10/04/2003

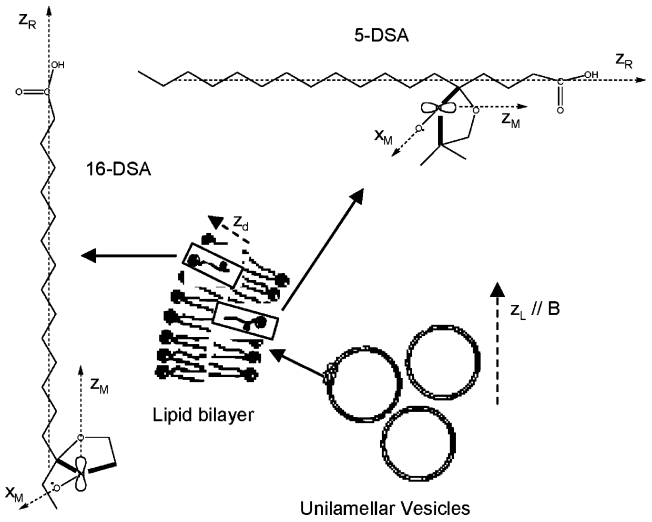

Figure 1. Molecular structures of 5- and 16-DSA spin probes and sketch of their location in the lipid bilayer of vesicles. Schematic representation of the axis systems used in the calculations of EPR spectra.

a stable nitroxide radical (n-doxyl stearic acid or n-DSA), which have been widely used as spin probes in natural and model membranes to obtain information on the fluidity of the lipid bilayer.[14−17] Two different kinds of spin probes, 5-DSA and 16-DSA, with the doxyl (4,4-dimethyl-N-oxy-oxazolidinyl) group in different positions of the acyl chain (Figure 1) were employed. In the case of 5-DSA, the doxyl moiety is five carbons away from the carboxyl headgroup. This spin probe therefore reports on the fluidity of lipids close to the polar headgroups of the bilayer. On the other hand, 16-DSA has its nitroxide moiety 16 carbons away from the headgroup of the stearic acid and reports on the lipid fluidity close to the bilayer core.

An accurate line shape analysis of the EPR spectra on the basis of Freed's theory of slow motional EPR[18,19] was performed using the microscopically ordered and macroscopically disordered (MOMD) model proposed by Meirovitch et al.[20,21] for ordered systems such as lipid bilayers. The differences found in dynamic and orientational ordering parameters between S and C samples were discussed in relation to the changes in lipid composition induced by copper stress.

To better understand the influence of lipid composition on the structure and dynamics of lipids in S and C vesicles, vesicles artificially enriched with specific lipids were also prepared and investigated by EPR spectroscopy. In particular, PM lipids from stressed plants were enriched with soy-PC and 16:0/18:1 PC (sample S+PC) to increase the PC/PE ratio and DBI to values similar to those of the control PM lipids. On the other hand, control lipids were enriched with 16:0/18:1 PE (sample C + PE) to obtain PC/PE ratio and DBI values similar to those of the S vesicles. In this case, the lowest PC/PE ratio that could be reached in stable vesicles was 0.4, with a DBI value of 1.7 (Table 1).

Experimental Section

Materials. Soybean PC, oleoyl-palmitoyl PC and PE, and n-DSA spin probes were purchased from Sigma-Aldrich (Steinhem, Germany). Solvents of analytical grade were from Merck (Darmstadt, Germany).

Wheat seedlings (*Triticum durum* Desf. cv. Creso) were grown for 11 days using nutrient solutions containing either 0.3 μM (control) or 50 μm Cu^{2+} (stressed), and root PMs were isolated with a two-phase aqueous polymer partition system, as reported in refs 5 and 13. Lipids were extracted from PMs as described in ref 5. For spin labeling, stock solutions of 5- and 16-DSA in ethanol (1 mg/mL) were prepared and added to the total lipid extracts in choloform to a label-to-lipid ratio of 1:100 (w/w). This ratio was chosen to obtain a satisfactory EPR signal quality avoiding spin−spin interactions between spin probes. Solvent was removed at room temperature under a stream of N_2. Large unilamellar vesicles (∅ 200 nm) were prepared in a 10 mM HEPES−NaOH buffer solution (pH 7.6) with an extrusion procedure as described in ref 13.

EPR Measurements. For EPR measurements, each vesicle suspension was transferred to a 100-μL capillary tube, which was sealed at both ends, inserted into a quartz sample holder, and put in the microwave cavity of the spectrometer. EPR spectra were recorded using a Varian (Palo Alto, CA) E112 spectrometer operating at X band, equipped with a Varian E257 temperature control unit and interfaced to a 100 MHz Personal Computer by means of an acquisition board[22] and a software package[23] especially designed for EPR and ENDOR experiments. Spectra were recorded every 5 K on temperature raising, waiting 10 min for equilibrating the temperature. For each spectrum, a field setting of 3265 G, a microwave power of 2 mW and a modulation amplitude of 0.5 G were employed. Spectra of 5-DSA and 16-DSA in a 10 mM HEPES−NaOH buffer solution (pH 7.6) were also performed in the same experimental conditions.

EPR Spectra Analysis. In all the investigated samples, EPR spectra of 5- and 16-DSA spin probes resulted from the superposition of two sub-spectra, a main sub-spectrum characteristic of radicals undergoing dynamics in the slow motion regime, and a minor sub-spectrum typical of radicals undergoing fast isotropic motion. The first sub-spectrum was ascribed to spin probes incorporated into the lipid bilayer of vesicles, while the second was assigned to probes free in the aqueous buffer. Different contributions of the last component to the spectra were observed depending on the sample and on the position of the doxyl group in the probe. In the case of 5-DSA in S and S + PC vesicles and of 16-DSA in all samples, the presence of the fast component hampered an accurate analysis of the spectral line shape when the NLSL fit program developed by Budil et al.[24] was used. In fact, the fitting procedure was scarcely sensitive to the minor component, which contributed to the spectral intensity for 3−5%. Thus, we separated the two components of the spectra by computer subtraction of the minor one prior to line shape analysis. The assumptions made were that, for each of the specimens, the spectrum of 5-DSA (or 16-DSA) in the buffer solution used for vesicle dispersion at room temperature (three lines, with a peak to peak width of 0.65 G and a line shape that can be well reproduced with a sum of a Lorentzian (45%) and a Gaussian (55%) function, separated by an isotropic nitrogen hyperfine coupling constant, a_N, of 15.7 G) was representative of the minor component at all temperatures, and its line shape was independent of temperature. The amplitude of the spectrum of 5-DSA or 16-DSA in the buffer solution was adjusted during subtraction until the peaks of the minor component of the complex spectrum were eliminated. The end point of the subtraction was determined by the disappearance of the low and high field peaks, with the difference spectrum appearing undistorted and exhibiting the correct line shape for the probe in a lipid bilayer.

The spectra of 5- and 16-DSA inserted in the vesicles, either directly recorded (5-DSA in C and C + PE samples) or obtained with the subtraction procedure (5-DSA in S and S + PC

samples, and 16-DSA in all the samples), were thus analyzed using the NLSL program,[24] where the dynamic parameters characterizing the molecular motion and the geometric and order parameters characterizing the molecular organization are obtained by a nonlinear-least-squares fit of the experimental spectrum to model calculations based on the stochastic Liouville equation.[19] Several frames of reference are defined in the slow motional spectra calculations (Figure 1). The first is the principal axis system (x_m, y_m, z_m) of the magnetic interactions, namely the g and hyperfine interactions, where it is assumed that $\boldsymbol{g}$ and $\boldsymbol{A}$ tensors are coaxial. By convention, the z_m axis is taken as lying along the nitrogen p orbital (or N−O π orbital) and the x_m axis is along the N−O bond.[18] The second is the rotational diffusion tensor frame (x_R, y_R, z_R) fixed on the spin probe molecule. The third is the director frame (x_d, y_d, z_d), which is the axis system relative to which the molecules orient in anisotropic fluids. We assumed this frame to be axially symmetric. The last one is the laboratory frame (x_L, y_L, z_L), in which the magnetic field lies along z_L. The relationships among these coordinate systems are specified by different sets of Euler angles. The MOMD model[20,21] was adopted (i.e., a model in which there are domains with local ordering but whose directors are isotropically distributed so that there is no macroscopic ordering). This model was proven to be suitable for describing order and dynamics in vesicles, model and natural membranes.[19−21,24] The microscopic orientational order is expressed by the order parameter S defined as[20,25]

$$S = \langle D_{00}^{2}(\theta)\rangle = \left\langle \frac{3\cos^2\theta - 1}{2} \right\rangle = \int P(\theta)\left(\frac{3\cos^2\theta - 1}{2}\right)\sin\theta\, \mathrm{d}\theta$$

where θ is the Euler angle defining the orientation of z_R with respect to z_d, $P(\theta)$ is the orientational distribution function given by

$$P(\theta) = \frac{\exp\left(\frac{1}{2}\lambda(3\cos^2\theta - 1)\right)}{\int \exp\left(\frac{1}{2}\lambda(3\cos^2\theta - 1)\right)\sin\theta\, \mathrm{d}\theta}$$

and λ is the dimensionless ordering potential that determines the extent of microscopic ordering. Beacause we deal with a vesicle dispersion, the radical reorients in bilayer fragments with local order but distributed with a random orientation in space. This corresponds to an integration of the spectral line shape over Ψ, the Euler angle between z_d and z_L, using a specified number of Ψ values. Here, calculations of 30 orientations were considered. The motion of the spin probe was described by a Brownian isotropic diffusion model characterized by the rotational diffusion coefficient R.

In the calculations, the following values were employed for the principal components of the $\boldsymbol{g}$ and $\boldsymbol{A}$ tensors: $g_{xx} = 2.0088$, $g_{yy} = 2.0061$, $g_{zz} = 2.0027$; $A_{xx} = 5.9$ G, $A_{yy} = 5.0$ G, $A_{zz} = 34.4$ G for 5-DSA; $A_{xx} = 5.1$ G, $A_{yy} = 4.7$ G, $A_{zz} = 32.6$ G for 16-DSA. Because the components of the $\boldsymbol{g}$ tensor cannot be reliably measured from the low-temperature X-band EPR spectra because of the broad lines, they were taken from the literature.[26] The principal components of the $\boldsymbol{A}$ tensor were determined from rigid limit EPR spectra of 5-DSA and 16-DSA in vesicles.

The calculation of the spectra was based on Lorentzian line shapes, which revealed to give more satisfactory results than Gaussian lines. A Lorentzian line width tensor (w_{xx}, w_{yy}, w_{zz}) was employed in the fit program,[24] with $w_{xx} = w_{yy} = w_{zz}$. Line widths used for calculating 16-DSA spectra ranged from 0.4 G at high temperatures to 1 G at low temperatures. As far as calculation of 5-DSA spectra is concerned, line widths ranging from 1 G at high temperatures to 2 G at low temperatures were employed, except for the spectrum of 5-DSA in S+PC vesicles at 273 K, for which a line width of 3 G was necessary.

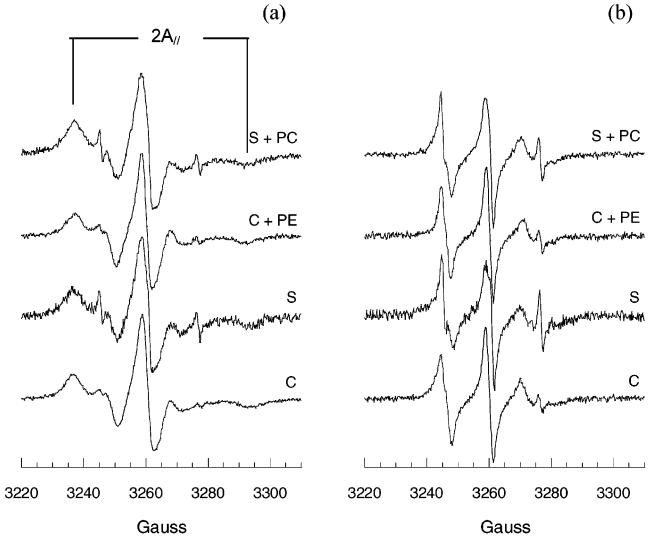

Figure 2. Experimental EPR spectra of (a) 5-DSA and (b) 16-DSA in samples C, S, C + PE, and S + PC at 293 K.

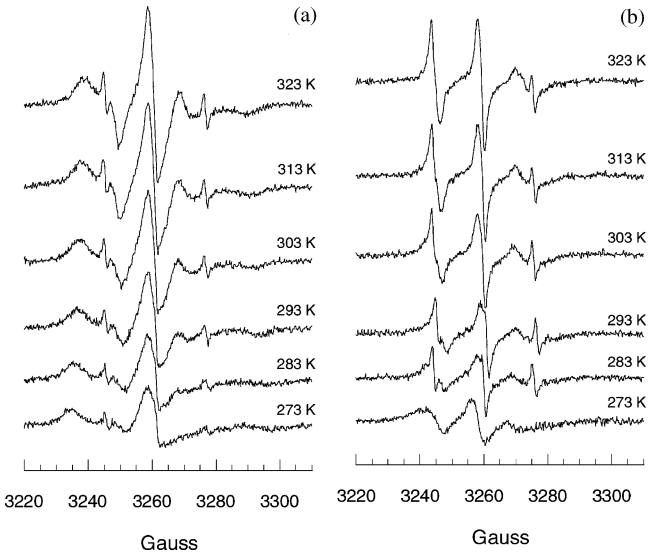

Figure 3. Experimental EPR spectra of (a) 5-DSA and (b) 16-DSA in sample S at the indicated temperatures.

Results and Discussion

Description of Spectra. Fluidity of C, S, C + PE and S + PC vesicles was investigated by probing the lipid chain mobility and ordering at two depths in the bilayers by using two stearic acids analogues, 5-DSA and 16-DSA, spin labeled 5 and 16 carbons away from the carboxyl headgroup, respectively (Figure 1). EPR spectra of 5-DSA and 16-DSA in vesicle samples were recorded over the temperature range between 273 and 323 K. Representative spectra are shown in Figures 2 and 3.

At any single temperature, differences in the spectral line shapes of 5-DSA and 16-DSA in the same sample (Figure 2) could be ascribed to the rotational mobility gradient typical of lipid bilayers when the nitroxide probe is placed further down the fatty acyl chain toward the center of the bilayer, from a relatively restricted polar head region to a more mobile terminal

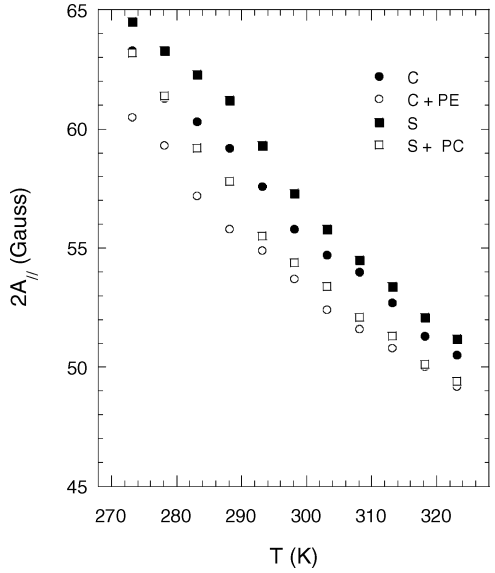

Figure 4. $2A_{||}$ values measured in the experimental EPR spectra of 5-DSA in samples C, S, C + PE, and S + PC. Errors are less than ± 0.4 G.

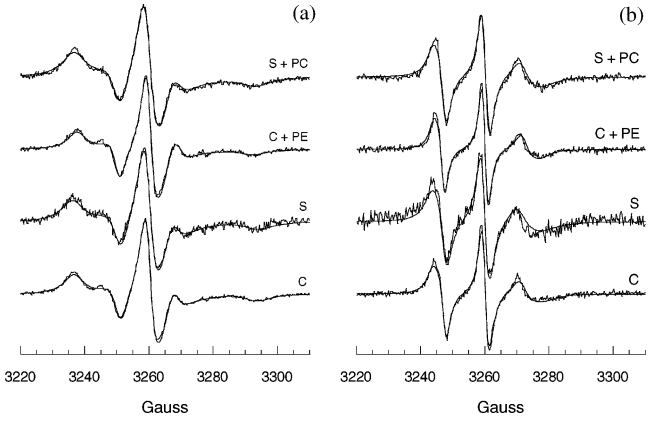

Figure 5. Experimental and best-fit calculated EPR spectra of vesicle-inserted (a) 5-DSA and (b) 16-DSA in samples C, S, C + PE, and S + PC at 293 K.

methyl region.[14−16,20,27] Moreover, a minor component with a line shape typical of spin probes undergoing fast isotropic motion appeared in all the spectra recorded above 273 K. This component had the same line shape at all the temperatures where it was observed, and it contributed to the spectral intensity of a given sample almost independently of temperature (Figure 3). The line shape was equal to that of 5-DSA or 16-DSA in the same buffer in which vesicles were dispersed (isotropic nitrogen hyperfine coupling constant $a_N = 15.7$ G). On the basis of these observations, the minor component was attributed to spin probes non absorbed by the vesicles and free in solution.[28] This component was not considered in the line shape analysis, which focused on EPR spectra of vesicle-inserted spin probes, obtained from the full spectra through the subtraction procedure described in the Experimental Section.

When the temperature was increased, a line shape evolution characteristic of an increasing mobility of the spin probes inside the lipid bilayer was observed for all the samples. Spectra of vesicle-incorporated 5-DSA showed high anisotropy, as typical for tight packing of lipids close to polar headgroups. In such spectra, the outer splitting $2A_{||}$ (Figure 4) can be considered as a measure of spin probe dynamics and acyl chain order in the vesicle bilayer. An increase in the value of $2A_{||}$ can be interpreted as a decrease in lipid fluidity. For all the samples, the trends of $2A_{||}$ with increasing the temperature reflect increases in 5-DSA mobility. No abrupt changes were observed in these trends, indicating that no neat phase transitions occur for our vesicles in the temperature range investigated.

When the EPR spectra of 5-DSA inserted in different lipid vesicles were compared at any single temperature, a different fluidity was revealed by both the spectral line shapes and the $2A_{||}$ splitting values. In particular, at room temperature (293−298 K), the lowest fluidity was shown by the S sample, indicating that lipids extracted from stressed wheat root plasma membranes form vesicles with more ordered molecular organization, in which molecular motions are reduced and acyl chains more tightly packed. A higher fluidity was found for lipids from control roots and S + PC vesicles, which showed a similar fluidity, whereas C + PE vesicles showed the highest fluidity. Spectra of 16-DSA in the bilayer showed enough anisotropy at low temperature (≤ 283 K), with the $2A_{||}$ splitting decreasing with increasing the temperature, whereas at higher temperatures (283−323 K), this anisotropy was no longer resolved, and three-line spectra appeared. In this case, the positions of spectral extremes were not very sensitive to motions, while the line widths decreased with an increase in temperature, indicating an increase in fluidity.

Line Shape Analysis of Vesicle-Inserted Spin Probes. The line shapes of slow motion EPR spectra were analyzed by applying a nonlinear least-squares fitting procedure, in which an isotropic Brownian rotational diffusion model for the molecular motion of the spin probes in an ordering potential was assumed (MOMD model[20,21]). As reported in the Experimental Section, a diffusion constant R describes the reorientational motion of the n-DSA doxyl moiety, whereas an order parameter S models the orientational ordering of the principal nitroxide axis system with respect to the local director. R and S values can thus be used to get quantitative information on vesicle fluidity (the reciprocal of viscosity), a term generally employed to describe the extent of disorder and the molecular motion (chain flexibility, reorientations, lateral diffusion) within a lipid bilayer. In this context, an increased fluidity can be related to a higher R value and/or a lower S value.

Satisfactory agreement between calculated and experimental spectra (as an example see Figures 5 and 6) was achieved with an orientational order parameter S progressively decreasing with increasing the temperature as shown in Figures 7a and 8a. For 5-DSA, S values ranged from 0.44 to 0.64, whereas values between 0.05 and 0.24 were obtained for 16-DSA. The calculated R parameters showed increasing trends with temperature for all the examined samples (Figures 7b and 8b), which can be satisfactorily described in terms of the Arrhenius equation $R = R^0 \exp(-E_a/RT)$, thus obtaining the activation energies reported in Table 2. R values ranged from $1.8\ 10^7$ to $1.4\ 10^8$ s^{-1} for 5-DSA and from $5.7\ 10^7$ to $2.1\ 10^8$ s^{-1} for 16-DSA. Moreover, higher activation energy values were found for the reorientational motions of 5-DSA with respect to 16-DSA, due to a higher sensitivity to temperature of the lipid chain part close to the polar headgroups.[29,30]

These results indicate that the doxyl group of 16-DSA, located in the bilayer core of the vesicles, experiences both a faster dynamics and a lower orientational order than that of 5-DSA, located in the hydrophilic part of the vesicles. This behavior is characteristic of spin labels attached to different positions of a lipid chain inserted in a fluid lamellar phase, where both a flexibility gradient and a tilt of the chain with respect to the bilayer normal are present.[29,31]

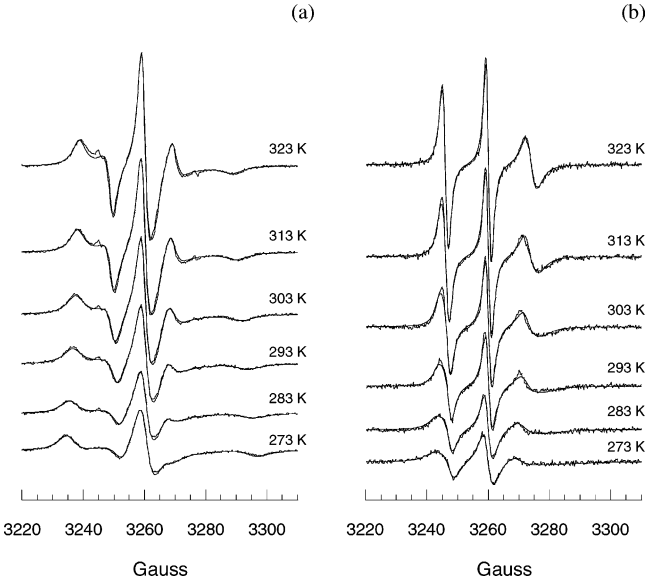

Figure 6. Experimental and best-fit calculated EPR spectra of vesicle-inserted (a) 5-DSA and (b) 16-DSA in sample C at the indicated temperatures.

TABLE 2: Activation Energies Determined Analyzing the Trends of Diffusion Coefficients *R* as a Function of Temperature in Terms of the Arrhenius Equation

sample	E_a (kJ/mol)
5-DSA	
C	28.3 ± 0.5
C + PE	21.9 ± 0.6
S	21.6 ± 0.5
S+PC	26.3 ± 0.5
16-DSA	
C	14.6 ± 0.6
C + PE	12.0 ± 0.5
S	12.2 ± 0.7
S+PC	12.3 ± 0.5

The location of the doxyl groups of 16- and 5-DSA in the bilayer is confirmed by the values of the isotropic nitrogen hyperfine coupling constant, $a_N = 1/3(A_{xx} + A_{yy} + A_{zz})$, found for the two spin probes by computer simulation of the relative rigid limit spectra. a_N is sensitive to the environmental polarity in the immediate vicinity of the spin label group.[16] We found that 5-DSA has $a_N = 15.1$ G, a value similar to that found for doxyl groups in aqueous solutions ($a_N = 15.7$ G in the buffer solution used here for vesicle dispersion), whereas 16-DSA has $a_N = 14.1$ G, a value closer to those found for n-DSA spin probes in heptane ($a_N \approx 14$ G). Therefore, the PM lipid vesicles here investigated display the characteristic profile of decreasing polarity toward the core of fluid bilayer membranes.[16]

Before discussing the *S* and *R* parameter values found for the different samples through the line shape analysis, we would like to comment on the reliability of the fit parameters on the basis of accuracy and correlation, and on the suitability of the model adopted in the fit procedure. The orientational order was described in the fitting program through the parameter λ (see Experimental Section). Errors up to 1% were found for this parameter in the calculations of all the analyzed spectra. The diffusion coefficient was determined in the fitting program as Log *R* with errors up to 0.1% for all the investigated samples. Correlation coefficients lower than 0.9 in absolute value were found between λ and Log *R* for all the analyzed spectra, indicating that a reliable individual determination of the fit parameters was performed in the procedure. However, errors on both parameters became bigger when considering the influence on the fit quality of the line width, a parameter kept constant in the procedure. In fact, the line width was found to be correlated to λ in most cases, and fittings performed using the components of the Lorentzian line width tensor as variable parameters gave unreliable results. Thus, we decided to keep w_{xx}, w_{yy} and w_{zz} fixed, and we run the fit procedure for different values of $w_{xx} = w_{yy} = w_{zz}$. Usually, fits with equally good spectral line shape reproduction were obtained with line width varying by up to ± 0.2 G. Therefore, errors on *S* and *R* were estimated in this way and reported in Figures 7 and 8.

As previously stated, the chosen model allowed a good agreement between experimental and calculated spectra to be obtained. In particular, the most significant spectral features, such as line positions and line shape evolution with temperature, were well reproduced (Figures 5 and 6). In some cases, a refinement of the model including a superposition of two or more spectra corresponding to sites with different values of *S* could have improved the reproduction of the line shapes.[20] n-DSA spin probes in vesicles experience both internal motions of the chain segments around the many C−C bonds and overall reorientation of the molecules within the bilayers.[32] X-band EPR spectra are, in principle, more sensitive to the overall tumbling than to the more rapid internal modes of motion.[33,34,35] Therefore, an axial diffusion tensor and the introduction of tilt angles between the magnetic and the diffusion principal axis frames could have given a physically more realistic description of the system, and possibly, a better line shape reproduction. On the other hand, EPR spectra of macroscopically unaligned membrane vesicles intrinsically have low resolution, reflecting the average behavior of the spin probes.[24,33,36] In fact, lipids in the bilayer are microscopically well aligned, but the macroscopic sample, composed of a vesicle dispersion, provides a random distribution of directions of alignment, defined by the directors, which are perpendicular to the bilayer plane (MOMD model). The superposition of spectra from all orientations results in a major source of inhomogeneous broadening that relates to the degree of microscopic ordering. This effect tends to mask the homogeneous broadening due to the molecular dynamics, rendering the MOMD spectra scarcely sensitive to details of different models.[24,36] The fit of our MOMD spectra was indeed barely affected by the adoption of a cylindrically symmetric rotational diffusion tensor, as well as by the introduction of a tilt angle between the magnetic and the diffusional principal axis frames. Moreover, the spectra contain insufficient information to permit unambiguous determination of all the parameters of an anisotropic rotational diffusion model. Therefore, in view of the fact that our simplified model gives a satisfactory reproduction of the line shapes as well as a good description of the effects of systematic variations in the experimental parameters (i.e., temperature and vesicle composition), and conscious of the fact that the simulations are most useful in interpreting trends rather than in their absolute significance,[36] for our purpose of directly comparing spectra of different samples, we decided to keep the model as simple as possible and to minimize the number of parameters in the fit. Thus, *R* and *S* can be considered as effective motional and local order parameters, respectively. To this purpose, it must be noticed that this model was successfully used in vesicle investigations by other authors.[28]

Effects of Copper Stress on PM Lipid Vesicle Fluidity. As reported above, the results of the line shape analysis indicated an analogous rotational dynamics and orientational ordering in all the investigated samples. In particular, the trends of both parameters with temperature agreed with a location of the spin probes in a tighter environment at lower temperatures. Moreover,

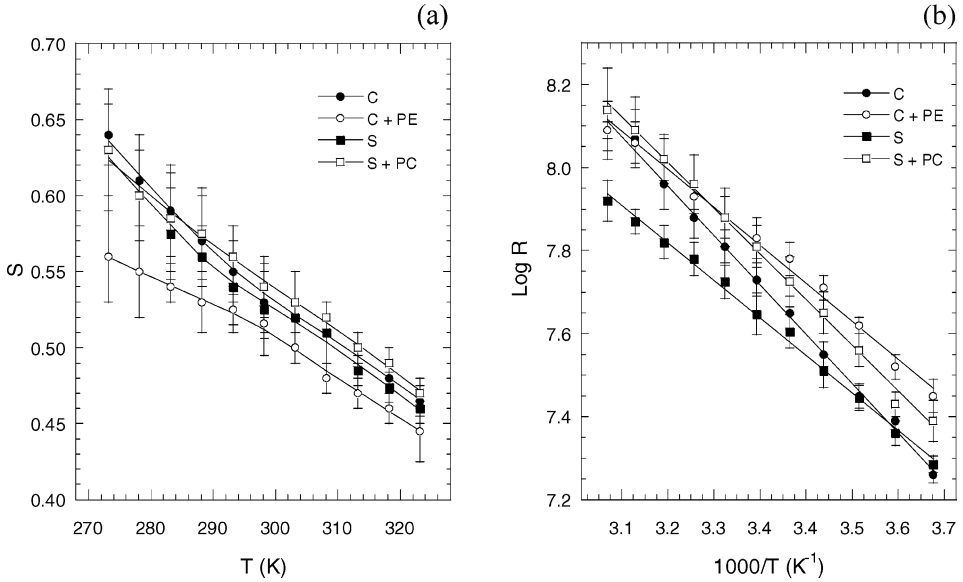

Figure 7. (a) Orientational order parameter (*S*) of 5-DSA in vesicles of samples C, S, C + PE, and S + PC as a function of temperature; lines are drawn to guide the eyes. (b) Log *R* vs 1000/*T* for the motion of 5-DSA in vesicles of samples C, S, C + PE, and S + PC; lines represent fits in terms of the Arrhenius equation.

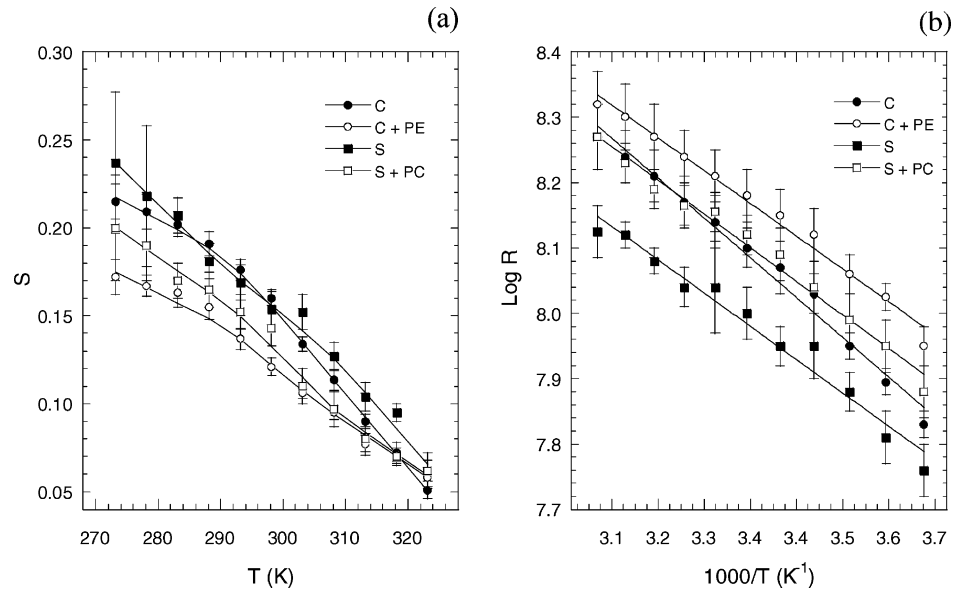

Figure 8. (a) Orientational order parameter (*S*) of 16-DSA in vesicles of samples C, S, C + PE, and S + PC as a function of temperature; lines are drawn to guide the eyes. (b) Log *R* vs 1000/*T* for the motion of 16-DSA in vesicles of samples C, S, C + PE, and S + PC; lines represent fits in terms of the Arrhenius equation.

a higher order degree and a more hindered dynamics were observed for 5-DSA with respect to 16-DSA in all samples at each temperature, as expected on the basis of the chain flexibility gradient described above.

Besides these analogies, significant differences in the fit parameters were detected in vesicles made of PM lipids from roots of control (C) and Cu-treated (S) wheat seedlings (Figures 7 and 8). In particular, both 5- and 16-DSA spin probes showed lower *R* values in S than in C vesicles, indicating a slowing down of the spin probe dynamics, affecting both the outer and the inner parts of the bilayer. Higher activation energies were found for the motion of the spin probes in the control with respect to the Cu-treated sample (Table 2), which can be related to a higher sensitivity of the control PM lipids to temperature changes. On the other hand, the Cu treatment scarcely affected the orientational ordering of the n-DSA spin probes in the PM lipid bilayer. In fact, very similar *S* values, within the experimental errors, were found for 5-DSA in C and S vesicles, whereas for 16-DSA, *S* was slightly higher in S than in C vesicles, due to a slightly tighter packing of the lipid chains in the hydrophobic core of the vesicle bilayer. These findings can be explained in terms of changes in PM lipid composition of roots induced by growth of wheat seedlings in Cu excess. (The main parameters describing lipid composition of vesicles are reported in Table 1; for more details see ref 5.) In fact, a higher percentage of phospholipids with shorter chains and a lower unsaturation degree (14:0 and 16:0 fatty acids increased, whereas 18:2 and 18:3 decreased following Cu stress[5]), as well as a lower PC/PE ratio are in agreement with a decreased bilayer fluidity.[10,30,37−41] A tighter packing of lipids in the bilayer is indeed favored by the substitution of choline with the smaller ethanolamine headgroups, which reduce repulsive forces in the hydrophilic part of the bilayer. On the other hand, repulsion between acyl chains in the inner core of the bilayer can be reduced by decreasing the length and the degree of unsaturation of lipid chains.[10,29,30,37,42,43] Moreover, a decrease in fluidity

could result from the ordering effect of membrane active sterols,[44] such as sitosterol, the main free sterol present in our plasma membranes.[5] In fact, though an increase in the PL/FS ratio was observed in the PM lipids following the copper treatment,[5] sterols might interact preferably with the more saturated and shorter chain phospholipids, thus favoring a tight packing of the membrane bilayer.[44]

Fluidity of Model Vesicles. Line shape analysis of 5- and 16-DSA EPR spectra in model vesicles S + PC and C + PE gave the *R* and *S* parameters reported in Figures 7 and 8. As it can be observed, in C + PE vesicles, the spin probes showed both faster rotational dynamics and lower orientational order than those in all the other samples. This behavior was observed for both 5- and 16-DSA, suggesting that the lipid composition of C + PE vesicles results in bilayers with high fluidity. In particular, the high degree of unsaturation of acyl chains, with a high content of unsaturated PEs, that is nonlamellar phase forming lipids,[10,30,37] could have caused a destabilization of the lipid bilayer packing. In S vesicles, the disordering effect of PE lipids is counteracted by the presence of shorter and more saturated acyl chains,[10,29,30,37] because highly unsaturated and long-chained PEs were found to form hexagonal phases, whereas short-chained PEs form lamellar phases.[42,43]

As far as S + PC vesicles are concerned, the 5-DSA doxyl group showed rotational diffusion coefficients very similar to those found for C + PE vesicles; however, values of *S* slightly higher than those found for C and S vesicles were obtained. For the doxyl group of 16-DSA in S + PC vesicles, a different behavior was observed. In fact, values of *S* and *R* intermediate between those obtained for C + PE and C samples resulted from the EPR line shape analysis. All these trends indicate that the addition of PC to S lipids has a fluidizing effects on the vesicles, which results in an increased rotational dynamics of the spin probes in both the outer and the inner parts of the lipid bilayer, but has a small ordering effect in the headgroup region and a disordering effect in the bilayer core. These results can be explained once again in terms of the different packing properties of PC with respect to PE headgroups and by the disordering effect of unsaturated chains on the lipid bilayer.[10,29,30,37−41]

Conclusions

In this study, we presented quantitative details on the fluidity changes in lipids from root PMs induced by growing wheat seedlings in excess copper. Quantitative information on orientational ordering and dynamics was obtained by analyzing the EPR spectra of 5-DSA and 16-DSA spin probes in large unilamellar vesicles made from PM lipids in terms of a microscopically ordered and macroscopically disordered model in which the probe reorientations were described as Brownian isotropic rotational diffusion. Small but significant differences were found in the simulation parameters *S* (the orientational order parameter) and *R* (the rotational diffusion coefficient) for vesicles S and C (i.e., vesicles made of lipids from stressed and control seedlings, respectively). In particular, a decrease in fluidity was observed for S samples with respect to C ones, which can be related to the alteration of PM lipid composition induced by Cu excess.[5] In this context, the reduced unsaturation degree and the accumulation of phospholipids with shorter acyl chains can be regarded as an adaptive strategy for root PM to better accommodate sterol molecules, which are primary elements in the regulation of membrane rigidity.[44] Moreover, a careful balance of lamellar-phase forming and hexagonal-phase forming lipids was observed in root PMs in response to Cu stress,[5] which preserves the lamellar liquid crystalline phase of the lipid bilayer at physiological temperatures.

This fine adjustment of lipid composition maintains the same permeability of membrane lipids to protons, while decreasing that to small molecules such as glucose.[7] Sustained proton gradients at the PMs of root cells are indeed essential for a selective ion uptake, and in perspective, for plant survival. On the other hand, a lower membrane fluidity, and consequently, permeability can be regarded as a defense against the penetration of harmful and toxic species. Similar results were observed for root plasma membranes of wheat[45] and *Spartina Patens*[46] under salinity stress.

Finally, model vesicles revealed to be useful in unraveling correlations between lipid composition, molecular interactions, and structural and dynamic properties of the PM lipid bilayer.

Acknowledgment. This study was financially supported by the University of Pisa (Fondi di Ateneo, 2002) and by MIPAF (Ministero delle Politiche Agricole e Forestali).

References and Notes

(1) Navari-Izzo, F.; Quartacci, M. F.; Pinzino, C.; Dalla Vecchia, F.; Sgherri, C. M. *Physiol. Plant.* **1998**, *104*, 630.

(2) Fernandes, J. C.; Henriques, F. S. *Bot. Rev.* **1991**, *57*, 246. Ciscato, M.; Valcke, R.; Van Loven, K.; Clijsters, H.; Navari-Izzo, F. *Physiol. Plant.* **1997**, *100*, 901. Maksymiec, W. *Phytosynthetica.* **1997**, *34*, 321. Quartacci, M. F.; Pinzino, C.; Sgherri, C. M.; Dalla Vecchia, F.; Navari-Izzo, F. *Physiol. Plant.* **2000**, *108*, 87. Hall, J. L. *J. Exp. Bot.* **2002**, *53*, 1.

(3) Van Assche, F.; Clijsters, H. *Plant Cell Environ.* **1990**, *13*, 195.

(4) De Vos, C. H. R.; Schat, H.; Voojis, R.; Ernst, W. A. O. *J. Plant Physiol.* **1989**, *135*, 164. De Vos, C. H. R.; Vonk, M. J.; Schat, H. *Plant Physiol.* **1992**, *98*, 853. De Vos, C. H. R.; Ten Bookum, W. M.; Vonk, M. J.; Voojis, R.; Schat, H.; De Kok, L. J. *Plant Physiol. Biochem.* **1993**, *31*, 151.

(5) Quartacci, M. F.; Cosi, E.; Navari-Izzo, F. *J. Exp. Bot.* **2001**, *52*, 77.

(6) Halliwell, B.; Gutteridge, J. M. C. *Biochem. J.* **1984**, *219*, 1. Aust, S. D.; Marehouse, L. A.; Thomas, C. E. *J. Free Rad. Biol. Med.* **1985**, *1*, 3. Stohs, S. J.; Bagchi, D. *Free Rad. Biol. Med.* **1985**, *18*, 321. Allen, R. D. *Plant Physiol.* **1995**, *107*, 1049. Sgherri, C.; Quartacci, M. F.; Izzo, R.; Navari-Izzo, F. *Plant Physiol.* **2002**, *40*, 591.

(7) Berglund, A. H.; Norberg, P.; Quartacci, M. F.; Nilsson, R.; Liljienberg, C. *Physiol. Plant* **2000**, *109*, 117.

(8) Meharg, A. A. *Physiol. Plant.* **1993**, *88*, 191.

(9) Hernandez, L. E.; Cooke, D. T. *J. Exp. Bot.* **1997**, *48*, 1375.

(10) Williams, E. E. *Am. Zool.* **1998**, *38*, 280.

(11) Navari-Izzo, F.; Rascio, N. In *Handbook of plant and crop stress*; Pessarakli, M., Ed.; Marcel Dekker Inc.: New York, 1999; pp 231−270.

(12) Berglund, A. H.; Quartacci, M. F.; Liljenberg, C. *Biochem. Soc. Trans.* **2000**, *28*, 905.

(13) Berglund, A. H.; Quartacci, M. F.; Calucci, L.; Navari-Izzo, F.; Pinzino, C.; Liljenberg, C. *Biochim. Biophys. Acta* **2002**, *1564*, 466.

(14) Hubbell, W. L.; McConnell, K. M. *J. Am. Chem. Soc.* **1971**, *93*, 314.

(15) Griffith, O. H.; Jost, P. C. In *Spin Labeling: theory and applications*; Berliner, L. J., Ed.; Academic Press: New York, 1976; Vol. 1.

(16) Marsh, D. In *Membrane Spectroscopy. Molecular Biology, Biochemistry, and Biophysics*; Gell, E., Ed.; Springer: Berlin, 1981; Vol. 31, pp 51−142.

(17) Gordon, L. M.; Curtain, C. C. In *Methods for studying membrane fluidity*; Aloia, R. C., Curtain, C. C., Gordon, L. M., Eds.; Alan R. Liss: New York, 1988; pp 25−88.

(18) Freed, J. H. In *Spin Labeling: theory and applications*; Berliner, L. J., Ed.; Academic Press: New York, 1976; Vol. 1.

(19) Schneider, D. J.; Freed, J. H. In *Biological Magnetic Resonance*; Berliner, L. J., Reuben, L. J., Eds.; Plenum: New York, 1989.

(20) Meirovitch, E.; Nayeem, A.; Freed, J. H. *J. Phys. Chem.* **1984**, *88*, 3454.

(21) Meirovitch, E.; Freed, J. H. *J. Phys. Chem.* **1984**, *88*, 4995.

(22) Ambrosetti, R.; Ricci, D. *Rev. Sci. Instrum.* **1991**, *62*, 2281.

(23) Pinzino, C.; Forte, C. *ESR-Endor*, Istituto di Chimica Quantistica ed Energetica Molecolare del Consiglio Nazionale delle Ricerche, 1992.

(24) Budil, D. E.; Lee, S.; Saxena, S.; Freed, J. H. *J. Magn. Reson. A* **1996**, *120*, 155.

(25) Zhang, J.; Luz, Z.; Zimmermann, H.; Goldfarb, D. *J. Phys. Chem. B* **2000**, *104*, 279.
(26) Gaffney, B. J. In *Spin Labeling: theory and applications*; Berliner, L. J., Ed.; Academic Press: New York, 1976; Vol. 1.
(27) Hoffman, P.; Sandhoff, K.; Marsh, D. *Biochim. Biophys. Acta* **2000**, *1468*, 359.
(28) Ottaviani, M. F.; Daddi, R.; Brustolon, M.; Turro, N. J.; Tomalia, D. A. *Langmuir* **1999**, *15*, 1973.
(29) Holte, L. L.; Peter, S. A.; Sinnwell, T. M.; Gawrisch, K. *Biophys. J.* **1995**, *68*, 2396.
(30) Gawrisch, K.; Holte, L. L. *Chem. Phys. Lipids* **1996**, *81*, 105.
(31) Moser, M.; Marsch, D.; Meier, P.; Wassmer, K.-H.; Kothe, G. *Biophys. J.* **1989**, *55*, 111.
(32) Cassol, R.; Ge, M.; Ferrarini, A.; Freed, J. H. *J. Phys. Chem. B* **1997**, *101*, 8782.
(33) Liang, Z.; Freed, J. H. *J. Phys. Chem. B* **1999**, *103*, 6384.
(34) Borbat, P. P.; Costa-Filho, A. J.; Earle, K. A.; Moscicki, J. K.; Freed, J. H. *Science* **2001**, *291*, 266.
(35) Lou, Y.; Ge, M.; Freed, J. H. *J. Phys. Chem. B* **2001**, *105*, 11053.
(36) Ge, M.; Freed, J. H. *Biophys. J.* **1999**, *76*, 264.
(37) Israelachvili, J. N.; Marčelja, S.; Horn, R. G. *Quart. Rev. Biophys.* **1980**, *13*, 121.
(38) Subczynski, W. K.; Wisniewska, A. *Acta Biochim. Pol.* **2000**, *47*, 613.
(39) McIntosh, T. J. *Chem. Phys. Lipids* **1996**, *81*, 117.
(40) Huster, D.; Jin, A. J.; Arnold, K.; Gawrisch, K. *Biophys. J.* **1997**, *73*, 855.
(41) Fenske, D. B.; Jarrell, H. C.; Guo, Y.; Hui, S. W. *Biochemistry* **1990**, *29*, 11222.
(42) Cullis, P. R.; De Kruijff, B. *Biochim. Biophys. Acta* **1978**, *513*, 31.
(43) Seddon, J. M.; Cevc, G.; Kaye, R. D.; Marsh, D. *Biochemistry* **1984**, *23*, 2634.
(44) Marsan, M. P.; Muller, I.; Milon, A. *Chem. Phys. Lipids* **1996**, *84*, 117. Hartmann, M. A. *Trends Plant Sci.* **1998**, *3*, 170. Barenholtz, Y. *Prog. Lipid Res.* **2001**, *41*, 1. Haines, T. H. *Prog. Lipid Res.* **2001**, *40*, 299.
(45) Mansour, M. M. F.; van Hasselt, P. R.; Kuiper, P. J. C. *Physiol. Plant.* **1994**, *92*, 473.
(46) Wu, J.; Seliskar, D. M.; Gallagher, J. L. *Physiol. Plant.* **1998**, *102*, 307.